Acta Acustica 2024, **8**, 61

https://doi.org/10.1051/aacus/2024058

Available online at:
https://acta-acustica.edpsciences.org

SCIENTIFIC ARTICLE OPEN ACCESS

Acoustic optimisation of the rail track by targeted variation of continuous superstructure parameters along the track

Maximilian Mantel*, Katja Stampka, and Ennes Sarradj

Department of Engineering Acoustics, Institute of Fluid Dynamics and Technical Acoustics, Technische Universität Berlin, Einsteinufer 25, 10587 Berlin, Germany

Received 8 April 2024, Accepted 27 August 2024

Abstract – Rolling noise is the dominant source for railway vehicles at medium train speeds. In order to reduce the contribution radiated by the rail, this paper investigates how structural irregularities affect sound propagation by varying the superstructure properties along a ballasted track. The so-called disorder is therefore used to optimise the track decay rate (TDR) and thus achieve a lower mean square velocity of the rail. Track parameters included in the analysis are the pad stiffness, the sleeper mass and the sleeper spacing. Structure-borne sound propagation in the rail is computed using a fast finite-difference method. Both periodically repeating and stochastically distributed variations are considered for parameter variation along the track, with up to three parameters being varied simultaneously. The most promising variation schemes are identified with the help of parameter optimisation using the brute-force method. It has been shown that a high TDR over a wider frequency range and a lower TDR drop in the pinned-pinned frequency range can be achieved due to the presence of disorder. The study indicates that variations of the superstructure parameters along the track are a promising method in order to reduce track vibration levels.

Keywords: Time-domain finite-difference method, Railway superstructure variation, Railway superstructure optimisation, Disorder

1 Introduction

The noise generated by rail vehicles can be attributed to various sources. In general, the primary noise sources include the engine and power units of the rail vehicle, the aerodynamic noise and the rolling noise. In the lower speed range up to 50 km/h, engine and aggregate noises predominate, whereas in the speed range from 50 to 250 km/h, rolling noises dominate and aerodynamic noises only from 250 km/h upwards [1]. This study's approach to reduce rolling noise emissions is limited to an active measure by modifying the superstructure. The main components of the track, and therefore the main opportunities for variation, are the rails, the sleepers, the pads, and the ballast. Each of these components affects the vibration behaviour of the rail in different frequency ranges [1].

The present work adopts the approach of modifying the superstructure by varying the superstructure properties, which lead to structural irregularities, also known as disorder. It is known that disorder has a major influence on sound propagation. For instance, it can result in the confinement of energy in the vicinity of the source. This phenomenon called Anderson localisation [2] limits the propagation of vibration at large distances from the location of excitation and is the subject of extensive research, which is comprehensively summarised by SenGupta [3]. For example, Pierre and Dowell [4] have shown that certain modes are perturbed in a small region when structural irregularities are present.

The track parameters of a conventional superstructure are generally considered to be approximately constant along the railway track. However, there are already indications that the targeted placement of structural irregularities along the track can influence rail vibrations. First, Heckl [5] analysed the influence of random sleeper spacing. It was shown that when the rail is excited in the region of the very dominant pinned-pinned frequency (half the wavelength of this frequency corresponds approximately to the sleeper spacing L_S), the deflection along the beam decreases faster with a high variation in sleeper spacing, but the deflection amplitude increases in the region of the excitation. A significant decrease in the mean square velocity, which is related to the sound radiation of the rail, was observed over a wide frequency range [5]. Subsequently, Nordborg [6] discussed the influence of track-support irregularities on the parametric excitation by a moving load mass. He concluded that a high degree of irregularity contributes to higher vibration levels up to 100 Hz. According to him, an optimisation

*Corresponding author: maximilian.mantel@tu-berlin.de

measure, such as a variation in pad stiffness, is not a suitable method to reduce noise. Furthermore, Wu and Thompson [7] considered the effects of random ballast stiffness and sleeper spacing along the track, as they inevitably occur in practical applications. According to them, one possible reason for different sleeper spacings is a lack of precision in the installation and an increase in deviations due to maintenance work. Furthermore, variations in ballast stiffness were mentioned to depend on the state of contact between the sleeper and the ballast. However, it was shown that random stiffness of the ballast only influences the frequency range below 300 Hz, whereas the random spacing of the sleepers affects the frequency range between 50 Hz and 1500 Hz. This was identified as the influence of the sleeper spacing on the effective sleeper mass, ballast and padding stiffness per unit length. Furthermore, it was observed that the pinned-pinned frequency is significantly reduced and sometimes even completely suppressed in some cases [7]. Abe et al. [8] carried out a further investigation to assess the effect of stochastically arranged sleepers according to a Gaussian distribution. The deflection amplitude at the excitation point was shown to decrease with significant variations in sleeper spacing during harmonic excitation of the pinned-pinned frequency. However, the opposite effect occurred with low variation, as higher amplitudes were obtained [8]. Batjargal et al. [9] conducted the only non-stochastic optimisation of various sleeper spacings. A transmission coefficient could be calculated using the model used. The researchers identified a nine-part sleeper group with different sleeper spacings, resulting in lower dominance of the pinned-pinned frequency than random sleeper spacings [9]. Additionally, a study by Abe et al. [10] compared the vibration behaviour of the nine-part sleeper group with two other random sleeper distributions and the resulting wheel-rail interaction. They confirmed a significant reduction in the amplitude of the rail deflection by using the optimal sleeper group. Nevertheless, when the perfectly periodic structure was disturbed, an increase in sound generation in the low-frequency range was observed during the interaction analysis [10].

These results indicate that variation of superstructure properties along the track can lead to an increased localisation of vibration, resulting in reduced structure-borne sound propagation. Therefore, this idea is extended by the variation of further superstructure properties and the investigation of additional variation schemes. In the following, the effects of different variations on the rail vibrational behaviour are analysed based on a numerical finite-difference method (FDM) model for calculating bending waves of an infinitely elastically supported beam [11]. An optimisation is performed, which considers the effects on the characteristic vibration parameters of the rail.

The remainder of the paper is organised as follows: First, the rail model with vibrational quantities and the finite-difference method is revisited. The method of this analysis is then described in detail, including the choice of the range of variation of the superstructure parameters, the optimisation criteria, the optimisation method, and the approach taken for parameter variation. Ultimately, the computational results are discussed and conclusions are drawn.

2 Rail model

Numerous models and methods for the simulation of rail vibrations are described in the literature; an overview can be found in [12]. The following sections investigate a ballasted track, which is a widely used track superstructure. For this type of track superstructure, it is assumed that the rail rests on the sleepers, with a pad between the sleepers and the rail. The sleepers are placed on ballast. Since the aim is to use a model that requires low computational effort, one of the most common models is used [1, 13] (see Fig. 1). This model only considers one rail whose vibration in the vertical direction is independent of the other rail. Pads and ballast are described by their spring stiffness and damping properties. A mass weighing half the sleeper mass m_s is considered to simplify the sleeper. According to [1, 11], the rail is approximated by an infinite Euler-Bernoulli beam, where the bending wave propagation is given by

$$\begin{aligned} EI_r \frac{\partial^4 u(x,t)}{\partial x^4} + m_r' \frac{\partial^2 u(x,t)}{\partial t^2} + d_r'(x) \frac{\partial u(x,t)}{\partial t} \\ = q(x,t) - s_\mathrm{p}(x)(u(x,t) - u_s(x,t)) \\ + d_\mathrm{p}(x)\left(\frac{\partial u(x,t)}{\partial t} - \frac{\partial u_s(x,t)}{\partial t}\right). \end{aligned} \tag{1}$$

The transverse deflection u depends on both x, the coordinate along the beam axis, and the time t. E is the rail Young's modulus, I_r is the rail cross-section area moment of inertia, and m_r' is the beam mass per unit length. q represents the excitation force per unit length and d_r is the viscous damping coefficient per unit beam length. s_p and d_p are the stiffness and the viscous damping coefficient of the pads. The transverse deflection of the sleeper u_s is given by

$$\begin{aligned} m_\mathrm{s}' \frac{\partial^2 u_\mathrm{s}(x,t)}{\partial t^2} = s_\mathrm{p}(x)u(x,t) - (s_b(x) + s_\mathrm{p}(x))u_\mathrm{s}(x,t) \\ + d_\mathrm{p}(x)\frac{\partial u(x,t)}{\partial t} - (d_\mathrm{p}(x) + d_\mathrm{b}(x)) \\ \times \frac{\partial u_\mathrm{s}(x,t)}{\partial t} \end{aligned} \tag{2}$$

with the stiffness s_b and the viscous damping coefficient d_b of the ballast.

No further assumptions are required to model the superstructure. Therefore, the superstructure can be arbitrarily varied along the rail.

The characteristic frequencies for a continuous two-layer model are described in Thompson et al. [1]. For the discrete rail model used, these characteristic frequencies can also be used as orientation. The resonance of the rail mass with the stiffness of the pad is thus described by $\omega_0 = \sqrt{\frac{s_\mathrm{p}}{m_r'}}$, whereby the frequency $\omega_1 = \sqrt{\frac{s_\mathrm{b}}{m_\mathrm{s}}}$ indicates the resonance of the sleeper mass with the stiffness of the ballast. Furthermore, an anti-resonance occurs at

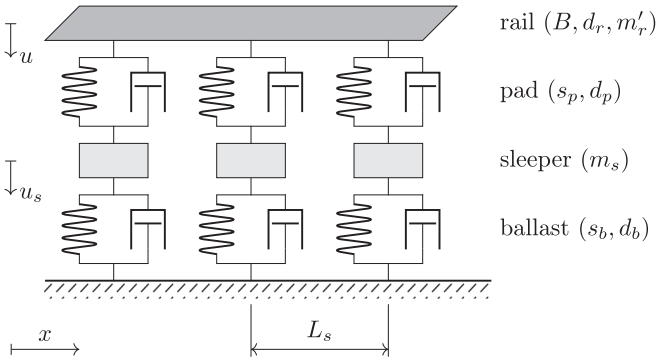

Figure 1. Two-layer elastic foundation model with discrete support.

$$\omega_2 = \sqrt{\frac{s_\mathrm{p} + s_\mathrm{b}}{m_\mathrm{s}}}. \tag{3}$$

The cut-off frequencies of this model are

$$\omega_{c1/2} = \sqrt{\frac{\omega_0^2 + \omega_2^2}{2} \pm \sqrt{\frac{\left(\omega_0^2 + \omega_2^2\right)^2}{4} - \omega_0^2 \omega_1^2}} \tag{4}$$

where almost no wave propagation below ω_{c1} and between ω_2 and ω_{c2} takes place [1]. Another relevant frequency is the so-called pinned-pinned frequency f_pp. Half the wavelength of this frequency corresponds approximately to the sleeper spacing L_S, resulting in almost unhindered propagation of the bending wave along the rail for this frequency [1].

2.1 Characteristic vibration quantities

To compare different track structures acoustically, it is useful to consider the decay behaviour of the bending waves along the track. According to standard EN 15461 [14], the track decay rate (TDR) can be used for this comparison. For this, a point input impedance is set in relation to transfer impedances, whose impact points are defined in the standard [14]. On the one hand, it is advantageous from an acoustic point of view if the TDR is as high as possible over a wide frequency range, as this ensures that the induced vibrations decrease rapidly along the track. A low TDR over a wider frequency range, on the other hand, has a disadvantageous effect. In contrast to the standard, frequency spectra rather than third-octave bands are used to analyse the TDR in this work, as a more precise analysis requires a better frequency resolution. In addition, only track decay rates in the vertical direction are considered.

Another quantity used to describe rail vibration is the mean square velocity (MSV), which has also been used by [5] and [7] in the study of random sleeper spacing. This frequency dependent quantity is defined by

$$\overline{v^2}(f) = \frac{1}{l - 2l_\mathrm{B}} \int_{l_\mathrm{B}}^{l-l_\mathrm{B}} |v(x,f)^2| \mathrm{d}x \tag{5}$$

and depends on the beam length l, the boundary length l_B and the spatial and frequency dependent beam velocity. In this study, the mean square velocity is averaged over the finite beam as a frequency dependent function. The boundary areas with length l_B are excluded, as no representative vibration behaviour of the rail can be expected in this region. In the application of the mean square velocity, it is assumed that this quantity is proportional to the radiated sound power [1]. The results of preliminary tests have indicated that, in certain instances, it may be beneficial to consider the mean squared velocity as an alternative or in conjunction with the track decay rate. In contrast to the track decay rate, an analysis is carried out at all local discretisation points of the beam. Furthermore, the track decay rate only describes the decay behaviour of the track vibration in contrast to the mean square velocity, which is proportional to the sound actually emitted [1]. It is similarly desirable to achieve the lowest possible mean square velocity value over a wide frequency range. In the following consideration, the MSV is used exclusively as a level value $\overline{L_v}$ with the reference velocity $v_0 = 5 \cdot 10^{-5} \frac{\mathrm{m}}{\mathrm{s}}$.

2.2 Finite-difference method (FDM)

To simulate the propagation of the bending vibrations along the infinite rail, the finite-difference method presented by Stampka and Sarradj [11] is applied. The model described in Section 2 is discretised to a uniform grid in space and time. The application of finite-differences allows the approximation of the derivatives in the equations of motion equations (1) and (2). A central finite-difference scheme of second-order accuracy is used to approximate the rail in space, while the implicit Crank-Nicolson method is utilised for the time approximation. This results in a system of equations which can be solved by specifying the deflections of the rail of the last two previous time steps or initial conditions in order to calculate the subsequent deflections for the next time step under a given force excitation. Further details of the method and the validation using analytical results can be found in [11].

In addition to several other models which enable the calculation of beam vibration with structural irregularities, this model is characterised particularly by its high computational efficiency. Taking into account the multitude of optimisation dimensions and the considerable range of variation delineated in Section 3.1, this property is of significant importance for the optimisation problem at hand.

3 Method

3.1 Superstructure parameters

In order to identify the most optimal superstructure designs, it is reasonable to limit the search space as much as possible. Consequently, the investigation focusses on the most influential superstructure properties. This means that only those structure properties that have the potential to contribute to a high TDR or low MSV level over a wide frequency range are considered. Furthermore, the variation of these properties must be practical for potential

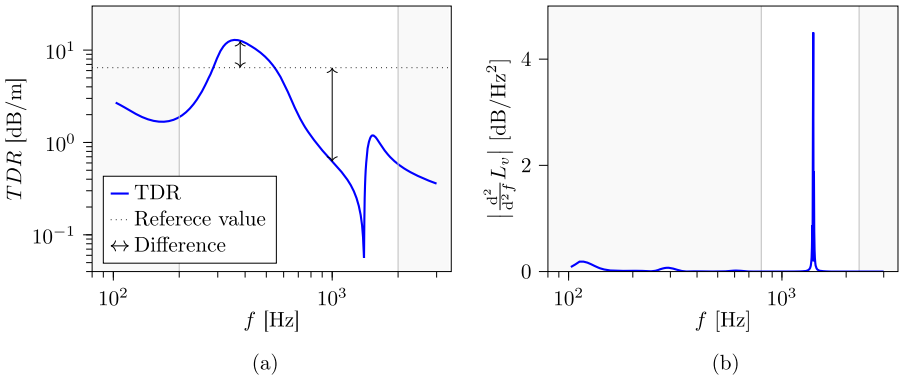

Figure 2. Clarification of the objective function approaches for optimising the TDR and the MSV according to the defined optimisation criteria. The grey area indicates the frequency ranges not considered. (a) TDR with deviation from a defined reference value. The objective function is calculated using the mean deviation within a defined frequency range. (b) Absolute value of the second degree derivative of the MSV level ($v_0 = 5 \cdot 10^{-5} \frac{\mathrm{m}}{\mathrm{s}}$). The objective function is calculated using the mean value within a defined frequency range.

implementation. The definition of the variation range should therefore be based on parameter values that can be found in practice.

The initial superstructure property to be examined is the stiffness of the pad, which has the potential to impact the blocked zone frequency limits in accordance with the resonant frequencies (Eqs. (3) and (4)). According to [1], the use of pads with different stiffness can be expected to influence the width of the blocked zone and thus contribute to the desired optimisation goal. The range of variation is defined based on practical parameter values taken from a series of measurements of Czolbe [15]. Since the specified static pad stiffness are of a comparable order of magnitude to dynamic values, these are used and limited to the variation range of 200 to 700 MN/s. The mean value of the variation range 450 MN/s represents the pad stiffness value of the reference superstructure. It can be assumed that an increased damping of the pad leads to a higher TDR in certain frequency ranges. However, the variation of the pad damping along the track is not expected to result in improved decay behaviour. Therefore, pad damping is not considered to be variable along the track.

The same approach to influence the blocked zone can be expected with the variation of the sleeper mass within a certain range according to the blocked zone frequency limits (Eqs. (3) and (4)). The initial reference value is defined by the conventional B 70 concrete sleeper, whose half-sleeper mass is 150 kg. The range of variation, which includes the weight of equally common B 58 and B 90 sleeper types, is therefore limited to 120–180 kg [16].

Additionally, the vibration behaviour of the rail can be modified by influencing the pinned-pinned frequency. This variable can be most significantly altered by modifying the sleeper spacing. In this case, it can be assumed that the pinned-pinned frequency is distributed over several frequencies due to the variation in sleeper spacings. The reference value is the sleeper spacing of 0.6 m used for conventional railway tracks [16]. According to Sañudo et al. [17], other sleeper spacings in the range of 0.5–0.7 m are also found in practice. It should be noted that the choice of the location increment Δx in the numerical method (Tab. A1) dictates that sleeper spacings are a multiple of Δx. Accordingly, the variation limits of the sleeper spacing in the analysis are 0.491 m and 0.709 m.

The variation of the ballast along the track is difficult to realise in practice. According to [1], the ballast stiffness and damping primarily affect the frequency range below 200 Hz and are, therefore, not the main determinants of the noise generated along the track. Thus, the properties of the ballast are not considered variable.

Changing the rail properties along the track seems impractical for safety and manufacturing reasons. Therefore, all rail parameters are chosen to be constant. All other constant values of the superstructure are listed in Table 1.

3.2 Optimisation criteria

In order to facilitate the optimisation process, it is necessary to evaluate and quantify the quality of all superstructure designs. For this purpose, two specific optimisation criteria are used to make a statement about an improvement. Accordingly, the first optimisation criterion is the width of the blocked zone and the second is the dominance of the pinned-pinned frequency. These two optimisation criteria have to be quantified using respective objective functions, which can later be optimised using an optimisation algorithm. The first objective function describes the average difference between the TDR values and a reference value R over the frequency range between $f_1 = 200$ Hz and $f_2 = 2000$ Hz (Fig. 2a). This reference value R is derived from the properties of the TDR reference curve, which is a non-variable reference superstructure whose properties were previously defined in Section 3.1. By calculating the mean value of the minimum and maximum value of the TDR reference curve within the frequencies f_1 and f_2, this value is $R = 6.45$ dB/m. This approach is used to widen

Table 1. Superstructure parameters for beam and non-variable superstructure properties.

Beam		
Beam bending stiffness	B	6.38 MN/m^2
Beam mass per unit length	m'_r	60.21 kg/m
Viscous damping coefficient per unit length	dr	1000 Ns/m^2
Superstructure		
Pad damping coefficient	d_p	33000 Ns/m
Pad stiffness coefficient	s_p	450 MN/m
Ballast damping coefficient	d_b	75000 Ns/m

the blocked zone during the optimisation process by minimising the objective function

$$F_1(\mathrm{TDR}) = \frac{1}{f_2 - f_1} \int_{f_1}^{f_2} |\mathrm{TDR}(f) - R| \mathrm{d}f. \tag{6}$$

Furthermore, the second objective function value calculates the mean absolute value of the second MSV level derivative over the influential frequency range of the pinned-pinned frequency from $f_3 = 800$ Hz to $f_4 = 2300$ Hz (Eq. (7)). The second derivative is used to determine the objective function value, as this strongly emphasises the influence of the pinned-pinned frequency and reduces the influence of the other frequency ranges (Fig. 2b).

$$F_2(\overline{L_v}) = \frac{1}{f_4 - f_3} \int_{f_3}^{f_4} \left| \frac{\mathrm{d}^2}{\mathrm{d}^2 f} \overline{L_v} \right| \mathrm{d}f. \tag{7}$$

3.3 Optimisation method

The optimisation method used is the brute force algorithm. This is a combinatorial approach that divides the search space into a regular grid. Each search space optimisation variable is assigned a grid factor N, which divides the defined variation range into N values. Only these values are used during the optimisation. When considering a single periodic variation of a superstructure property, the defined grid factors result in a total quantity M of superstructure states by means of the definition of a period length n_p using the equation

$$M = N^{n_\mathrm{p}}. \tag{8}$$

Each of these states can be assigned an objective function value via the defined objective functions, which can be used to assess the quality of the superstructure. Accordingly, all objective function values of the corresponding variation scheme are compared during optimisation, with the state exhibiting the lowest objective function values considered the optimum [18, 19]. The same procedure is used to vary different superstructure properties, but different grid factors are applied.

3.4 Variation approach

Different variation schemes are taken into account during the optimisation process. A basic distinction is made between the variation of a single superstructure property (S), the pairwise variation of two superstructure properties (P), and the joint variation of all superstructure properties (T). For single and pair variations, periodic and stochastic variation approaches are analysed. Finally, the results of single and pair variations are to be specifically combined in the overall variation.

Table 2. Grid factors N_s for all analysed period lengths for the periodic single variation of the superstructure properties selected in Section 3.1.

	N_s				
n_p	**2**	**3**	**4**	**5**	**6**
s_p	20	10	8	6	5
m_s	20	10	8	6	5
d_s	5	5	5	5	5

3.4.1 Single variation (periodic)

In the case of a periodic single variation, different grid factors are assigned to different period lengths. Consequently, the grid factors are chosen to ensure that the total number of superstructure designs remains within a range that leads to an acceptable computational effort. The selected grid factors can be found in Table 2. For example, in the variation approach of the periodically varying pad stiffness, the grid factor $N = 5$ is selected for the period length $n_\mathrm{p} = 6$. Consequently, the pad stiffness can have five different values at each of the six sleeper positions within a period. This results in a total of $M = 15{,}625$ different superstructure designs for this variation scheme according to equation (8).

As can be seen in Table 2, the grid factor for the variation in sleeper spacing is $N = 5$ for all the periods mentioned. This is due to the fact that the sleeper spacings can only assume discrete values anyway due to the numerical discretisation of the rail, and therefore all possible sleeper spacings within the defined period range can be covered with this factor.

When evaluating a superstructure, it must also be taken into account that, with varying superstructure properties, the rail vibration behaviour is strongly dependent on the location of the excitation. On the one hand, this is due to the fact that the superstructure properties in the surrounding area of the excitation are particularly decisive for calculating the TDR. Furthermore, because of the discretisation of the beam, the location of the excitation is not exactly in

the centre of a sleeper compartment and changes with different sleeper spacing variations. When periodic variations are implemented, the superstructure is excited at all centres of the sleeper compartments, with a subsequent average of the respective results. Accordingly, the corresponding objective function value is only calculated after averaging the two vibration quantities for all runs. This approach necessitates an increased number of calculation runs.

A closer look at the total number of superstructure designs M to be calculated shows that the required averaging results in some superstructure designs that correspond to redundant results. It can therefore be assumed that mirroring a period will result in an identical objective function value due to the intended averaging. If the start of the period is phase-shifted, this also leads to redundant results due to the excitation at all sleeper centres. Consequently, combinations that lead to redundant results can be excluded. The total quantity from the previous example of the periodic variation of the pad stiffness at period $n_\mathrm{p} = 6$ is reduced from $M = 15{,}625$ to $M_\mathrm{red} = 2635$ by neglecting all redundant superstructure designs.

3.4.2 Single variation (stochastic)

When performing stochastic variations, a Gaussian distribution is used whose expectation value represents the respective reference value. Likewise, no values outside the variation limits specified in Section 3.1 are allowed. All stochastic variations are given the grid factor $N = 20$, which gradually increases the variation range of the standard deviation from zero to the parameter variation limit. Since the parameter values of the corresponding superstructure properties around the point of excitation in particular influence the vibration behaviour of the rail, the distribution of the most influential superstructure components does not correspond to a Gaussian distribution due to the insufficient number. In order to reduce the random influence, the vibration behaviour of 2000 randomly generated superstructures is averaged for each standard deviation value.

3.4.3 Pairwise variation (periodic)

In the case of periodic pair variation, the period length for the joint periodic variation of several superstrucutre properties is assumed to be the same, and thus the total number of superstructure designs is $M = (N_1 \cdot N_2)^{n_\mathrm{p}}$. This assumption is used to limit the search space and thus save computing capacity. An example of a superstructure with several varying superstructure properties with a defined period length is shown in Figure 3. The grid factors for all period lengths analysed can be found in Table 3. For example, the grid factors $N_{s_\mathrm{p}} = 3$ and $N_{m_\mathrm{s}} = 3$ are defined for the periodic variation of the pad stiffness and the sleeper mass for the period length $n_\mathrm{p} = 4$. This means that both pad stiffness and sleeper mass can have three different values at all four sleeper positions. This leads to $M = 6561$ different superstructure variants, whereby after subtracting all variants that lead to redundant results, only $M_\mathrm{red} = 1665$ need to be calculated.

Since the maximum period length of the combinatorial approach is limited to $n_\mathrm{p} = 4$ so far, an extension is planned to allow investigating larger periods. In the case where two superstructure properties with $n_\mathrm{p} \leq 4$ were previously investigated and yielded only two parameter values each, it can be assumed that this also applies to longer periods. In this particular instance, additional period lengths can be investigated by setting the grid factors to $N_1 = N_2 = 2$, whereby no regular grid is required.

A further simplification can be derived from the parameter pairs that appear in the results with a shorter period. Thereby, for example, the case can arise that a certain hard pad always appears with a specific low sleeper mass or a certain soft pad always appears with a specific high sleeper mass. When the period length is extended to $n_\mathrm{p} > 4$, the grid factors remain $N_1 = N_2 = 3$. However, this results in a reduction in the number of possible superstructure designs, since the parameters associated with the pairs must still appear as pairs.

3.4.4 Pairwise variation (stochastic)

The pairwise stochastic variation of two structural properties follows the same procedure as single stochastic variation. The grid factor still corresponds to $N = 20$ for both superstructure properties. This means that the variation ranges of both superstructure properties are divided into twenty possible standard deviations. The relative standard deviation in relation to the respective maximum standard deviation is constant for both superstructure properties. Consequently, only twenty superstructure designs are examined for each pair.

3.4.5 Total variation

Following the completion of single and pair variations, the results can be employed to vary all three superstructure properties. Combinations of stochastic and periodic superstructure properties are also permitted. This signifies that the rail vibration is averaged with respect to both the excitation across all sleeper centres and the random recalculation with 2000 repetitions of the stochastic parameter values.

4 Results and discussion

Overall, a total of 43 different variation schemes were examined and the optimal result from each variation scheme was selected. In order to explain the effects of varying the single superstructure properties alone, the optimal results for all variation schemes analysed for the single variations are presented first. The results from the most successful variation schemes of the single variations are then presented together with the best schemes of the pair and total variations. All numerical parameters used in the calculations are listed in Table A1.

The optimised variation schemes for the single variation in pad stiffness are shown in Figure 4a. These were

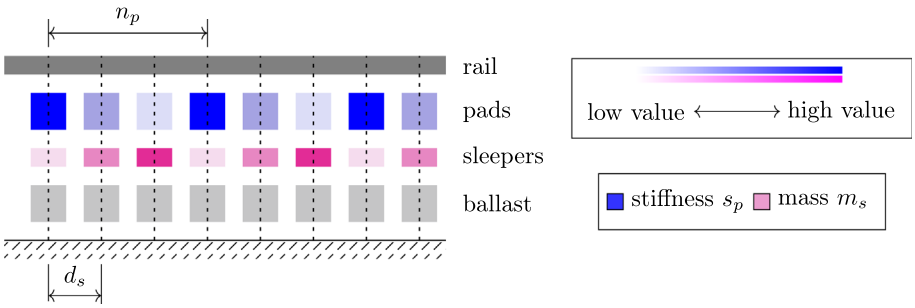

Figure 3. Example of variation scheme for a periodic change of the pad stiffness and the sleeper mass with same period length $n_\mathrm{p} = 3$. The representation of the superstructure is based on the superstructure model described in Figure 1. The degree of colour transparency is directly proportional to the parameter value indicated on the colour scale.

Table 3. Grid factors ($N_{s,1}$, $N_{s,2}$) for pairwise periodic variation of two superstructure properties with corresponding period lengths.

	($N_{s,1}$, $N_{s,2}$)		
n_p	**2**	**3**	**4**
(s_p, m_s)	(10, 8)	(5, 5)	(3, 3)
(m_s, d_s)	(12, 5)	(5, 5)	(3, 3)
(s_p, d_s)	(12, 5)	(5, 5)	(3, 3)

optimised according to the first optimisation criterion. A significant extension of the blocked zone can be achieved by varying only the pad stiffness. The optimal superstructure designs of the periodic variations mix very soft and very hard pads (Tab. B1). This is reasonable because analytical resonance frequencies (Eqs. (3) and (4)) for constant stiffness suggest that soft pads shift the lower boundary of the blocked zone into the lower frequency range and hard pads shift the upper boundary of the blocked zone into the higher frequency range using hard pads. However, the widening of the blocked zone is accompanied by a reduction in the TDR peak.

However, when considering the optimised variation schemes according to the first optimisation criterion for the periodic sleeper mass variation (Fig. 4b), the widening of the blocked zone does not occur, but the TDR peak still decreases slightly. Despite the exclusive appearance of the extreme values 120 kg and 180 kg (Tab. B2) in the optimal designs, there is no significant widening of the blocking zone.

The optimised variation schemes with respect to the second optimisation criterion for the periodic sleeper spacing show the expected behaviour (Fig. 4c). For the optimal designs, the pinned-pinned frequency dip is divided into several dips and is less dominant. The second optimisation criterion is met accordingly. The resulting parameter values are again almost solely limit values of the specified value range (Tab. B3). However, there are no decisive effects on the blocked zone range. This result is very similar to the study by Batjargal et al. [9]. Although the range of variation for the periodic variation of sleeper spacing was smaller, only the smallest and largest possible sleeper spacing values appeared. By modifying the superstructure, it was possible to reduce the degree of transmission and thus significantly reduce the rail vibration in the frequency range around the pinned-pinned frequency.

The best candidates from the stochastic variation of a single superstructure property are shown in Figure 4d. The evaluation by the corresponding objective function was carried out according to the same assignment as for the previous periodic variations. The best result is obtained with the highest reduction in the dominance of the pinned-pinned frequency at the maximum standard deviation. However, the only effective stochastic variation is the sleeper spacing variation. In this case, the pinned-pinned frequency dip in the resulting TDR curve is not split into several dips, as with periodic variation. Instead, the dip loses dominance and appears as an apparent attenuation. The study by Heckl [5] also showed a reduced manifestation of the pinned-pinned frequency dip, but this was divided into several clearly visible peaks and dips. However, it must be taken into account that a different numerical model was used and the probability distribution did not resemble a Gaussian distribution. In contrast, the study by Wu and Thompson [7] used a Gaussian distribution which, as in this study, resulted in a comparable behaviour of the TDR around the pinned-pinned frequency. However, it was found that a small deviation resulted in an increase in deflection at the excitation point and only larger deviations resulted in a reduction. Such a negative effect on the objective function value with a low standard deviation is not apparent in this investigation. The comparison of Abe et al. [10] between the investigation already mentioned of the ideal periodic sleeper spacing of Batjargal et al. [9] and the effect of the stochastic sleeper spacing variation of Abe et al. [8] should also be considered. The results indicated that the periodic variation was more effective than the stochastic variation. This is inconsistent with the findings of this study, which indicate that stochastic variation in sleeper spacing is more effective than periodic variation.

Compared to the stochastic variation of the pad stiffness and the sleeper mass, the results for the corresponding periodic variations were better able to meet the optimisation criteria. For these superstructure properties, it can be

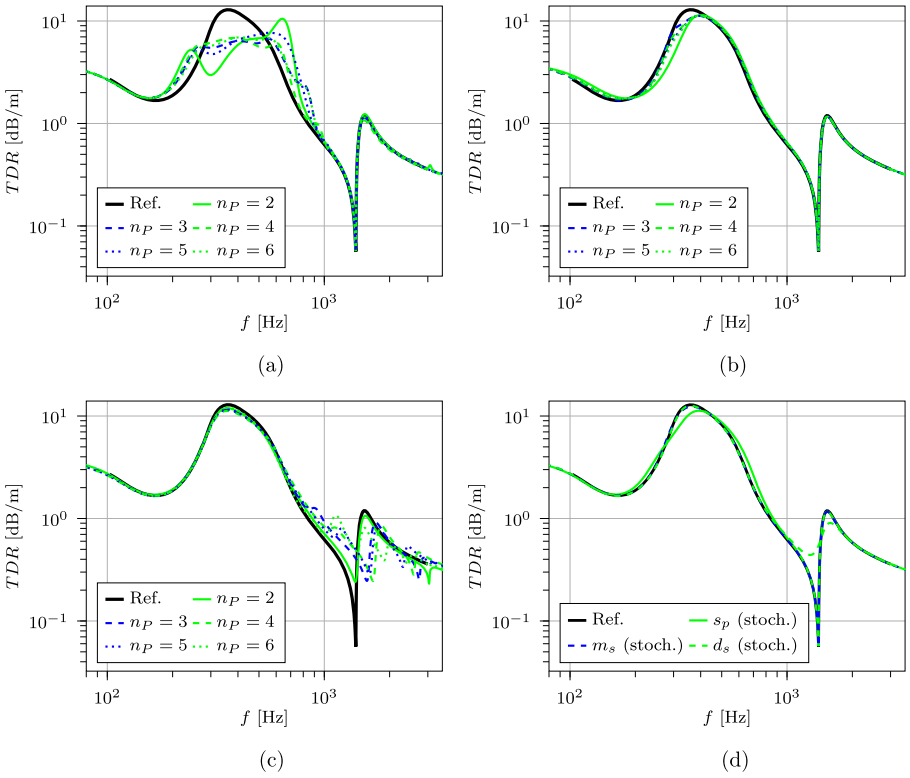

Figure 4. Resulting TDRs for optimised variation schemes for single variations: Stochastic variation of the sleeper spacing. (a) Periodic variation of pad stiffness. (b) Periodic variation of sleeper mass. (c) Periodic variation of sleeper spacing. (d) Stochastic variation of all three superstructure properties with the standard deviations $\sigma_{s_p} = 223.7$ MN/s, $\sigma_{m_s} = 26.8$ kg and $\sigma_{d_s} = 0.109$ m.

stated that the correlated disorder approach leads to a more desirable rail vibration behaviour than with uncorrelated disorder. This has already been observed in other studies, such as the investigation of correlated disorder in rainbow metamaterials by Fabro et al. [20].

In the following, the most successful variation schemes of the single variations are compared with those of the pairwise and total variation. The best optimised variation schemes of the entire study are listed in Table 4. All superstructure variation schemes of the pair and total variation were evaluated according to the first target criterion

The optimal result from the pairwise periodic variation of the pad stiffness and the sleeper mass ($P1_{\mathrm{opt}}$) leads to a further widening of the blocked zone compared to the periodic variation of the pad stiffness ($S1_{\mathrm{opt}}$) alone (Fig. 5). This indicates that the analytical relationship (Eqs. (3) and (4)) is effective, as a high pad stiffness with a low sleeper mass and a low pad stiffness with a high sleeper mass often result. Due to the occurrence of certain pairs of parameters, the duration of the period could be extended to $n_{\mathrm{p}} = 8$ in the investigation, as described in Section 3.4.

The optimal result for the pairwise periodic variation of pad stiffness and sleeper spacing ($P2_{\mathrm{opt}}$) shows that both optimisation criteria can be influenced (Fig. 5). This results in an extension of the blocked zone and a decrease in the dominance of the pinned-pinned frequency. The parameter values again consist almost exclusively of the limit values (Tab. B5). Thus, as described in Section 3.4, the assumption was made that only these limit values may occur for the period lengths $n_{\mathrm{p}} > 4$, which allowed an extension to the period length $n_{\mathrm{p}} = 7$.

The last variation scheme includes the periodic variation of the pad stiffness and the sleeper mass, as well as the stochastic variation of the sleeper spacing (Fig. 5, $T1_{\mathrm{opt}}$). This varies all selected superstructure properties, building on the previous results. Since the periodic variation in pad stiffness and sleeper spacing ($P2_{\mathrm{opt}}$) showed that both optimisation criteria can be influenced independently of each other, it can be assumed that this also applies to the combination of the variation of all three superstructure properties. The periodic variation schemes of pad stiffness and sleeper mass were re-examined for $n = 2\ldots8$ with a stochastically varying sleeper spacing at the maximum standard deviation. In addition to meeting both optimisation criteria, further widening of the blocking zone can be observed compared to $P2_{\mathrm{opt}}$.

Finally, when looking at Figure 5, it is not clear which of the superstructure designs leads to the best rail vibration behaviour. In general, the designs $P1_{\mathrm{opt}}$, $P2_{\mathrm{opt}}$, and $T1_{\mathrm{opt}}$ give good results. However, which of these designs could be used in practice depends on the corresponding boundary conditions and requirements.

In summary, it can be stated that the effects of disorder described by SenGupta [3] are also evident in the present results. Thus, it can be assumed that the presence of structural irregularities serves to concentrate the energy

Table 4. Overview of the best variation schemes (S: single variation, P: pairwise variation, T: total variation): The number of actual calculation runs when neglecting redundant results is given as M_{red}.

Acronym	Number of varied parameters	Parameters and variation form		Criteria	n_{p}	M_{red}
		Periodic	Stochastic			
$S1_{\mathrm{opt}}$	1	s_{p}		1	6	2635
$S2_{\mathrm{opt}}$	1	m_{s}		1	5	1560
$S3_{\mathrm{opt}}$	1	d_{s}		2	6	2635
$S4_{\mathrm{opt}}$	1		d_{s}	2	/	20
$P1_{\mathrm{opt}}$	2	$s_{\mathrm{p}} + m_{\mathrm{s}}$		1	6	60
$P2_{\mathrm{opt}}$	2	$s_{\mathrm{p}} + d_{\mathrm{s}}$		1	5	208
$T1_{\mathrm{opt}}$	3	$s_{\mathrm{p}} + m_{\mathrm{s}}$	d_{s}	1 + 2	8	7

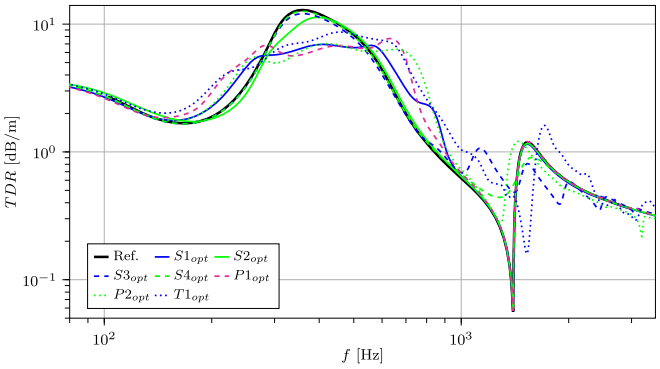

Figure 5. Overall comparison of all resulting TDRs of optimal results from Table C1.

at the site of excitation, thereby exerting a positive influence on the TDR. In addition, the optimisation of all variation schemes led to the frequent occurrence of limit values within the specified variation ranges. This result is consistent with the observations of Cha and Pierre [21], who demonstrated that the degree of localisation is dependent on the strength of disorder.

Generally, varying superstructure properties have some practical implications that need to be considered if such a design is to be implemented. According to Dahlberg [22], variations in stiffness along the superstructure lead to faster track wear and therefore higher maintenance and life cycle costs. It should also be noted that according to Sol-Sánchez et al. [23], hard pads generally protect the fastening system due to lower rail deflections and reduce energy loss during the journey, but also contribute to higher stiffness fluctuations and faster track wear. Soft pads, on the other hand, reduce stiffness fluctuations but lead to higher energy loss during the journey. The effect of combining soft and hard pads on non-acoustic aspects remains uncertain. Furthermore, the use of low sleeper masses must be carefully considered. According to Fendrich and Fengler [24], a sleeper mass that is too low can lead to insufficient resistance to track displacement, which in the worst case can result in track distortion. Therefore, safety aspects must be taken into account. In addition, a greater construction effort is also expected when building the track with variable parameters.

5 Conclusion

In this work, the effects of structural irregularities in the superstructure on structure-borne noise reduction were analysed. The investigation of correlated and uncorrelated disorder through the periodic and stochastic variation of the superstructure properties was able to show the potential of possible noise reduction measures. It was shown that periodic variation of the pad stiffness can achieve a significant widening of the TDR blocked zone. Furthermore, the periodic variation in sleeper mass demonstrated only minor effects. The dominance of the pinned-pinned frequency could also be clearly influenced by the periodic and stochastic variation in sleeper spacing. In the case of the periodic variation, the pinned-pinned frequency dip was divided into several less pronounced dips. In addition, an apparent attenuation occurred in the case of stochastically varied sleeper spacing, which significantly mitigated the dip. The combined variation of several superstructure properties also showed that the blocked zone and the surrounding area of the pinned-pinned frequency can be independently influenced. Thus, the periodic variation of the pad stiffness and of the sleeper spacing resulted in a widening of the blocked zone and a simultaneous reduction of the dominance of the pinned-pinned frequency. In conclusion, the approach of introducing disorder by varying one or more superstructure properties along the track can be regarded as an effective method for enhancing the decay behaviour of the rail.

Acknowledgments

We acknowledge support by the Open Access Publication Fund of TU Berlin.

Conflicts of interest

The authors declare no conflict of interest.

Data availability statement

Data are available on request from the authors.

References

1. D. Thompson: Railway noise and vibration: mechanisms, modelling and means of control, Elsevier, Oxford, UK, 2008. https://doi.org/10.1016/B978-0-08-045147-3.X0023-0.

2. P.W. Anderson: Local moments and localized states, Reviews of Modern Physics 50, 2 (1978) 191–201. https://doi.org/10.1103/RevModPhys.50.191.
3. G. SenGupta: Effects of deviations from periodicity, in: G. SenGupta (Ed.), Vibration of periodic structures, Elsevier, Oxford, UK, 2024, pp. 177–187. https://doi.org/10.1016/B978-0-32-399022-6.00018-7.
4. C. Pierre, E. Dowell: Localization of vibrations by structural irregularity, Journal of Sound and Vibration 114, 3 (1987) 549–564. https://doi.org/10.1016/S0022-460X(87)80023-8.
5. M.A. Heckl: Railway noise – can random sleeper spacings help?, Acta Acustica United with Acustica 6 (1995) 559–564.
6. A. Nordborg: Parametrically excited rail/wheel vibrations due to track-support irregularities, Acta Acustica United with Acustica 84, 5 (1998) 854–859.
7. T.X. Wu, D.J. Thompson: The influence of random sleeper spacing and ballast stiffness on the vibration behaviour of railway track, Acta Acustica United with Acustica 86 (2000) 313–321.
8. K. Abe, S. Batjargal, K. Koro: Resonant behavior of railway track having random sleeper spacing, Advances in Structural Engineering and Mechanics (2013) 1903–1912.
9. S. Batjargal, K. Abe, K. Koro: Sleeper spacing optimization for vibration reduction in rails, Journal of the Computational Structural Engineering Institute of Korea 25, 6 (2012) 569–577. https://doi.org/10.7734/coseik.2012.25.6.569.
10. K. Abe, S. Batjargal, K. Koro: Influence of sleeper spacing on vibration and noise of railway tracks, ISMA 26 (2014) 3385–3396.
11. K. Stampka, E. Sarradj: A time-domain finite-difference method for bending waves on infinite beams on an elastic foundation, Acoustics 4 (2022) 867–884. https://doi.org/10.3390/acoustics4040052.
12. A.C. Lamprea-Pineda, D.P. Connolly, M.F. Hussein: Beams on elastic foundations – a review of railway applications and solutions, Transportation Geotechnics 33 (2022) 100696. https://doi.org/10.1016/j.trgeo.2021.100696.
13. A. Nordborg: Wheel/rail noise generation due to nonlinear effects and parametric excitation, Journal of the Acoustical Society of America 111, 4 (2002) 1772–1781. https://doi.org/10.1121/1.1459463.29.
14. Railway applications – Noise emission – Characterisation of the dynamic properties of track sections for pass by noise measurements – EN 15461:2008+A1, CEN Bruessels, 2008.
15. C. Czolbe: Akustisch optimierte Schienenzwischenlage – Schlussbericht, Technical report, PROSE AG, Winterthur, Switzerland, 2020.
16. R. Menius, V. Matthews: Railway construction and infrastructure. 10th edn., Springer Vieweg Wiesbaden, Wiesbaden, 2020. https://doi.org/10.1007/978-3-658-27733-8.
17. R. Sañudo, M. Cerrada, B. Alonso, L. dell'Olio: Analysis of the influence of support positions in transition zones. A numerical analysis, Construction and Building Materials 145 (2017) 207–217. https://doi.org/10.1016/j.conbuildmat.2017.03.204.
18. H. Tolle, Optimization methods, Springer, Berlin, Heidelberg, 1975. https://doi.org/10.1007/978-3-642-87731-5.
19. P. Virtanen, R. Gommers, T.E. Oliphant, M. Haberland, T. Reddy, D. Cournapeau, E. Burovski, P. Peterson, W. Weckesser, J. Bright, S.J. van der Walt, M. Brett, J. Wilson, K.J. Millman, N. Mayorov, A.R.J. Nelson, E. Jones, R. Kern, E. Larson, C.J. Carey, I. Polat, Y. Feng, E.W. Moore, J. VanderPlas, D. Laxalde, J. Perktold, R. Cimrman, I. Henriksen, E.A. Quintero, C.R. Harris, A.M. Archibald, A. H. Ribeiro, F. Pedregosa, P. van Mulbregt: SciPy 1.0 contributors, SciPy 1.0: fundamental algorithms for scientific computing in python, Nature Methods 17 (2020) 261–272. https://doi.org/10.1038/s41592-019-0686-2.
20. A. Fabro, H. Meng, D. Chronopoulos: Correlated disorder in rainbow metamaterials for vibration attenuation, Proceedings of the Institution of Mechanical Engineers, Part C: Journal of Mechanical Engineering Science 235, 14 (2021) 2610–2621. https://doi.org/10.1177/0954406220986596.
21. P.D. Cha, C. Pierre: Vibration localization by disorder in assemblies of monocoupled, multimode component systems, Journal of Applied Mechanics 58, 4 (1991) 1072–1081. https://doi.org/10.1115/1.2897684.
22. T. Dahlberg: Railway track stiffness variations – consequences and countermeasures, International Journal of Civil Engineering 8, 1 (2010) 1–12.
23. M. Sol-Sánchez, F. Moreno-Navarro, M.C. Rubio-Gámez: The use of elastic elements in railway tracks: a state of the art review, Construction and Building Materials 75 (2015) 293–305. https://doi.org/10.1016/j.conbuildmat.2014.11.027.
24. L. Fendrich, W. Fengler: Handbook of railway infrastructure. 3rd edn., Springer Vieweg, Berlin, Heidelberg, 2019. https://doi.org/10.1007/978-3-662-56062-4.

Appendix A

FDM parameters

Table A1. Parameters of the FDM simulation performed. All defined parameters are explained in [11].

Calculation end time	t_{end}	0.4	s
Time increment	Δt	$2 \cdot 10^{-5}$	s
Grid parameter	b	1.058	–
Local step size	Δx	0.0545	m
Theoretical rail length (without boundaries)	l	80	m
Number of boundary grid points	n_{B}	600	–
Force parameter	σ	$0.5 \cdot 10^{2}$	s
Force parameter	a	$0.7 \cdot 10^{-4}$	–

Appendix B

Optimised superstructure designs with different variation schemes

Table B1. Parameters of the optimised superstructure designs with periodically varying pad stiffness at the corresponding period length n_p. The optimisation was carried out according to the first optimisation criterion.

n_p	Prop	Sleeper positions								Unit
		1	**2**	**3**	**4**	**5**	**6**	**7**	**8**	
1		450 (Reference)								
2		226	700			...				
3		256	311	700			...			
4		271	342	271	700			...		
5	s_p	200	300	700	300	700		...		MN/s
6		200	325	700	325	325	700		...	
7		200	200	325	325	700	325	700	...	
8		200	325	700	325	325	700	200	700	

Table B2. Parameters of the optimised superstructure designs with periodically varying sleeper mass at the corresponding period length n_p. The optimisation was carried out according to the first optimisation criterion.

n_p	Prop	Sleeper positions						Unit
		1	**2**	**3**	**4**	**5**	**6**	
1		150 (Reference)						
2		120	120			...		
3		120	120	180		...		
4	m_s	120	120	120	180		...	kg
5		120	120	120	120	180	...	
6		120	120	120	120	120	180	

Table B3. Parameters of the optimised superstructure designs with periodically varying sleeper spacing at the corresponding period length n_p. The optimisation was carried out according to the second optimisation criterion.

n_p	Prop	Sleeper positions						Unit
		1	**2**	**3**	**4**	**5**	**6**	
1		0.6 (Reference)						
2		0.491	0.709			...		
3		0.491	0.491	0.709		...		
4	d_s	0.491	0.491	0.491	0.709		...	m
5		0.491	0.491	0.491	0.6	0.709	...	
6		0.491	0.491	0.491	0.709	0.709	0.709	

Table B4. Parameters of the optimised superstructure designs with periodically varying pad stiffness and sleeper mass in pairs. The optimisation was carried out according to the second optimisation criterion.

n_p	Prop.	Sleeper positions								Unit
		1	**2**	**3**	**4**	**5**	**6**	**7**	**8**	
1	s_p	450 (Reference)								MN/s
	m_s	150 (Reference)								kg
2	s_p	255.6	700	...						MN/s
	m_s	171.4	137.1							kg
3	s_p	200	450	700	...					MN/s
	m_s	180	180	120						kg
4	s_p	200	450	450	700	...				MN/s
	m_s	180	120	180	120					kg
5	s_p	200	200	700	450	700	...			MN/s
	m_s	180	180	120	180	120				kg
6	s_p	200	700	450	450	200	700	...		MN/s
	m_s	180	120	180	180	180	120			kg
7	s_p	200	450	450	450	700	200	700	...	MN/s
	$m\mathrm{s}$	180	120	180	180	120	180	120		kg
8	s_p	200	200	450	450	700	700	200	700	MN/s
	m_s	180	180	180	180	120	120	120	120	kg

Table B5. Parameters of the optimised superstructure designs with periodically varying pad stiffness and sleeper spacings in pairs. The optimisation was carried out according to the second optimisation criterion.

n_p	Prop.	Sleeper positions							Unit
		1	**2**	**3**	**4**	**5**	**6**	**7**	
1	s_p	450 (Reference)							MN/s
	d_s	0.709 (Reference)							m
2	s_p	700	700	...					MN/s
	d_s	0.491	0.709						m
3	s_p	200	200	700	...				MN/s
	d_s	0.491	0.709	0.491					m
4	s_p	200	200	700	700	...			MN/s
	d_s	0.491	0.709	0.491	0.491				m
5	s_p	291	291	291	700	700	...		MN/s
	d_s	0.709	0.709	0.709	0.491	0.491			m
6	s_p	291	291	291	291	291	700	...	MN/s
	d_s	0.709	0.709	0.709	0.491	0.491	0.491		m
7	s_p	291	291	700	291	700	291	700	MN/s
	m_s	0.491	0.709	0.491	0.709	0.491	0.709	0.709	m

Table B6. Parameters of the optimised superstructure designs of the total variation consisting of the periodic pair variation of the pad stiffness and the sleeper mass as well as the parallel stochastic variation in the sleeper spacing using $\sigma = 0.109$ m. The optimisation was carried out according to the first optimisation criterion.

n_p	Prop.	Sleeper positions								Unit
		1	**2**	**3**	**4**	**5**	**6**	**7**	**8**	
1	s_p	450 (Reference)								MN/s
	m_s	150 (Reference)								kg
	d_s	0.6 (Reference)								m
4	s_p	200	450	450	700					MN/s
	m_s	180	120	180	120		⋯			kg
	d_s	0.6 ($\sigma = 0.109$ m)								m
6	s_p	200	700	450	450	200	700			MN/s
	m_s	180	120	180	180	180	120	⋯		kg
	d_s	0.6 ($\sigma = 0.109$ m)								m
7	s_p	200	450	450	450	700	200	700		MN/s
	m_s	180	120	180	180	120	180	120	⋯	kg
	d_s	0.6 ($\sigma = 0.109$ m)								m
8	s_p	200	200	450	450	700	700	200	700	MN/s
	m_s	180	180	180	180	120	120	180	120	kg
	d_s	0.6 ($\sigma = 0.109$ m)								m

Appendix C

Overview of best designs

Table C1. Parameter values of the superstructure designs with the most successful variation schemes; the corresponding vibration quantities are shown in Figure 5 and the associated variation schemes of the corresponding acronyms can be found in Table 4.

Acronym	Prop.	Sleeper positions								Unit
		1	**2**	**3**	**4**	**5**	**6**	**7**	**8**	
$S1_{opt}$	s_p	200	325	700	325	325	700	⋯		MN/s
$S2_{opt}$	m_s	120	120	120	120	180		⋯		kg
$S3_{opt}$	d_s	0.491	0.491	0.491	0.709	0.709	0.709	⋯		m
$S4_{opt}$	d_s	0.6 ($\sigma = 0.109$ m)								m
$P1_{opt}$	s_p	200	700	450	450	200	700	⋯		MN/s
	m_s	180	120	180	180	180	120			kg
$P2_{opt}$	s_p	291	291	291	700	700		⋯		MN/s
	d_s	0.709	0.709	0.709	0.491	0.491				kg
$T1_{opt}$	s_p	200	200	450	450	700	700	200	700	MN/s
	m_s	180	180	180	180	120	120	180	120	kg
	d_s	0.6 ($\sigma = 0.109$ m)								m

Cite this article as: Mantel M. Stampka K. & Sarradj E. 2024. Acoustic optimisation of the rail track by targeted variation of continuous superstructure parameters along the track. Acta Acustica, **8**, 61. https://doi.org/10.1051/aacus/2024058.